Iterative Tuning of Linear Quadratic Controller for AMBs in a High Speed Compressor

Se Young Yoon* and Zongli Lin
Dept. of Electrical and Computer Engineering
University of Virginia
Charlottesville, VA 22904, U.S.A.

Paul E. Allaire
Dept. of Mechanical and Aerospace Engineering
University of Virginia
Charlottesville, VA 22904, U.S.A.

Abstract

This paper presents the design of an Active Magnetic Bearing (AMB) rotor radial levitation controller using an iterative tuning method developed for the Linear Quadratic Gaussian (LQG) design problem. An iterative method is used to find the ideal pair of state and input weights in the LQG objective function that result in the best performance and stability robustness characteristics of the closed-loop AMB system. A search method is used to identify a set of input weight and state weight pairs that result in AMB levitation controllers that satisfy the necessary requirements for digital implementation. Furthermore, the stability and performance requirements from the API 617 and ISO 14839 standards for new compressors with AMB support are included in the controller design process. Finally, the derived LQG rotor levitation controller is implemented on a high speed centrifugal compressor test rig with a rigid rotor. Experimental results are presented and compared to the measurements obtained with a preliminary PID controller. The measured unbalance response and rotor orbit plots demonstrate the benefits of the proposed LQG method.

1 Introduction

Active magnetic bearings (AMBs) are non-contact bearings used in compressors and other rotating machines. The AMBs levitate the spindle within the bearing clearance by balancing the attractive forces generated by electromagnets acting at opposite sides of the rotor. By precise control of the currents to the electromagnets, the rotor is allowed to move freely and without any mechanical contact with the static components. Consequently, the AMBs eliminate the need of oil or other lubricants in the bearing, allowing the machine to operate cleanly and virtually maintenance free for longer periods of time. Additionally, these contactless bearings allow machines such as compressors and motors to be coupled directly and operate at high speeds without parasitic frictional losses. This also eliminates the need of complicated gear drives and creates an overall more reliable system.

One of the most important limitations of AMBs in commercial applications has involved the design and implementation of the stabilizing controller. AMBs are open loop unstable systems, and require a feedback controller for operation. Although advanced control algorithms have been developed in the literature to exploit the full capacity of AMBs, they are in many cases ignored in industrial applications because they are considered highly intricate to design and implement. On the other hand, simple and easily configurable controllers such as PID are largely preferred in commercial systems. Some of the key aspects concerns in AMB systems that have been studied in the literature include the stabilization of systems subjected to large external disturbances using classical [1, 2, 3] and advanced control methods [4, 5, 6], and systems on flexible or non-static structure. The control of an AMB suspended rigid rotor for space application was studied in [7] and [8]. The control of AMB systems for rotating machines with waving foundation was studied in [9].

A simple but effective optimal controller that is popular in many real-world applications is the Linear Quadratic Gaussian (LQG) controller. Among other advantages, the LQG controller results in good transient characteristics of the closed-loop system. A review of the implementation of LQG

*syy5b@virginia.edu

control methods in AMB systems can be found in [10]. An LQG controlled system was presented in [11] where a system identification algorithm automatically tunes the LQG controller based on the observed model uncertainty. Combinations of AMB nonlinearity compensation method with LQG controllers were studied [12] and [13]

This paper presents the design of an AMB rotor radial levitation controller using an iterative tuning method developed for the LQG controller. The proposed iterative method is used to find the ideal pair of state and input weights in the LQG objective function that result in the best performance and stability robustness characteristics of the closed-loop AMB system. A brief review of the objective and design procedure of linear quadratic regulator (LQR) and LQG controllers is provided in Sect. 2. An AMB supported compressor test rig is introduced in Sect. 3. The iterative tuning method of the LQG controller is described in Sect. 4 through the design of the AMB levitation controller of the centrifugal compressor test rig. The designed levitation controller is synthesized to satisfy the existing API 617 and ISO 14839 standards for new compressors with AMB support. The derived LQG rotor levitation controller is implemented on a high speed centrifugal compressor test rig, and experimental results are presented in Sect. 5. The performance of the AMB levitation system with the LQG controller is compared to the measurements obtained with a preliminary PID controller, which was manually tuned for initial levitation and testing of the AMB system.

2 Linear Quadratic Gaussian Controller

The Linear Quadratic Gaussian (LQG) regulator is one of the most common optimal control schemes for linear time-invariant systems, and a detailed discussion of the theory can be found in [14]. In this section we briefly review the objective and design procedure of this linear quadratic optimal controller.

Assume that we are given the following state space representation of a linear time-invariant (LTI) system with state and output noises,

$$\dot{x}(t) = Ax(t) + Bu(t) + w, \tag{1a}$$

$$y(t) = Cx(t) + Du(t) + v, \tag{1b}$$

where x is the state vector, u is the input vector, y is the output vector, and (A,B) is a controllable pair of state and input matrices. The external inputs w and v are the state and the measurement noises, which are assumed to be Gaussian white noise signals with the covariance matrix,

$$W_{\mathrm{n}} = \mathrm{E}\left\{ \begin{bmatrix} w \\ v \end{bmatrix} \begin{bmatrix} w^{\mathrm{T}} v^{\mathrm{T}} \end{bmatrix} \right\}, \tag{2}$$

where E stands for the expected value. The objective of the LQG design problem is to find an output feedback controller $K_{\mathrm{LQG}}(s)$, which minimizes the quadratic cost function J_{LQG},

$$J_{\mathrm{LQG}} = \mathrm{E}\left\{ \lim_{T\to\infty} \int_0^T \left(x^{\mathrm{T}} Q x + u^{\mathrm{T}} R u \right) \mathrm{d}t \right\}. \tag{3}$$

The resulting LQG regulator is a combination of an optimal state feedback controller to minimize J_{LQG} and an optimal Gaussian observer that estimates the system states for the given noise covariance matrix. The state feedback controller minimizing J_{LQG} is known as the linear quadratic regulator (LQR). The structure of the LQG controller is illustrated in the closed-loop block diagram in Fig. 1. The Matlab function *lqg* in the Control System Toolbox is employed in the design of the LQG rotor lateral suspension controller presented in this paper.

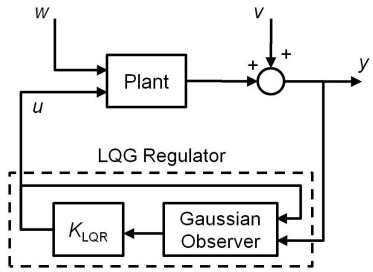

Figure 1: LQG controller structure.

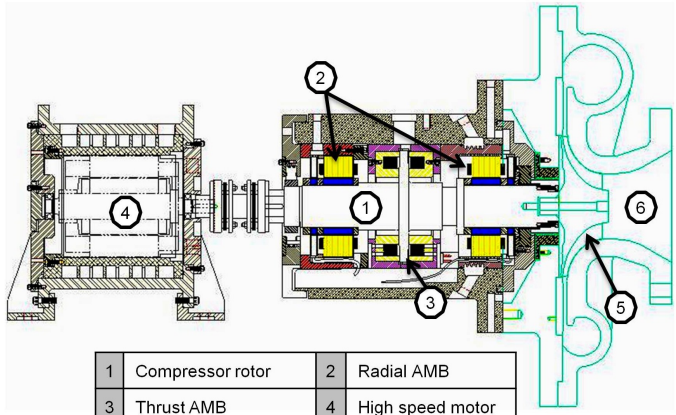

1	Compressor rotor	2	Radial AMB
3	Thrust AMB	4	High speed motor
5	Unshrouded impeller	6	Inlet

Figure 2: Unshrouded single stage centrifugal compressor with a vaneless diffuser, an electric motor and a rotor supported on active magnetic bearings.

3 Description of the Compressor Test Rig

In this paper we consider the AMB supported high speed centrifugal compressor shown in Fig. 2, which was built at the University of Virginia for the study of compressor surge. The maximum operating speed of the compressor is 17,000 rpm, limited by the motor variable frequency drive. The rotor shown in Fig. 3 has a total length of 0.517 m and mass of 27 kg. Two AMBs, which are identified in Fig. 2 as motor-side (MS) at the left-hand end and compressor-side (CS) at the right-hand end of the bearing housing, provide radial support of the rotor.

The lateral dynamics of the rotor is modeled using finite element methods, and the resulting model is reduced in order by employing modal truncation. The lateral resonance modes of the free-free rotor is plotted in Fig. 3, where the first four modes were included in the rotor model. The first free-free critical speed was found to be at 40,792 rpm, with a separation margin of 140% above the compressor maximum continuous operating speed, and the second critical speed is placed at 93,865 rpm. Therefore, the rotor in this system is considered to be rigid within the compressor operating speed range in order to simplify the AMB controller design process.

As illustrated in Fig. 2, two radial AMBs stabilize the lateral dynamics of the rotor. A general AMB rotor suspension system is shown in Fig. 4. With bias currents of 4 A and 3 A corresponding

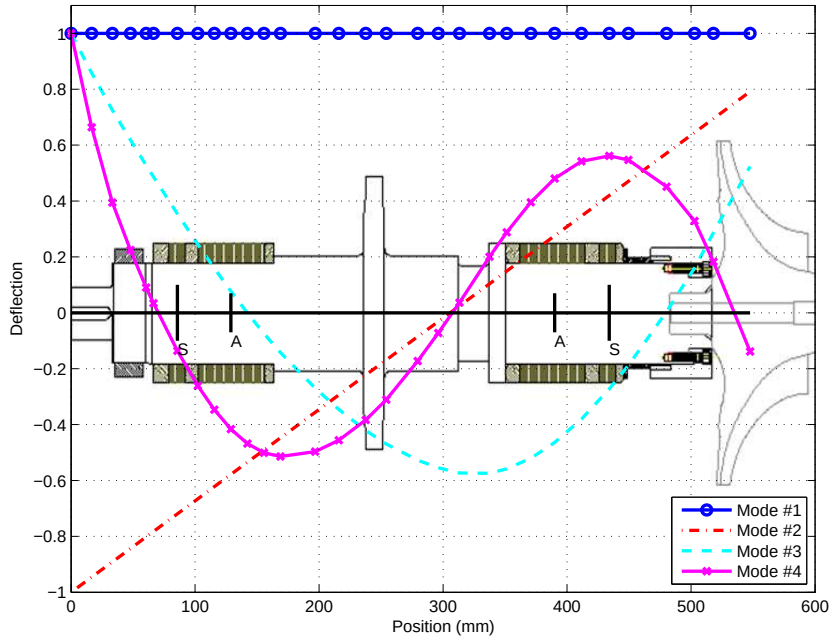

Figure 3: Resonance mode shapes for the free-free rotor. Sensor locations are marked with "S," and AMB actuators are marked with "A."

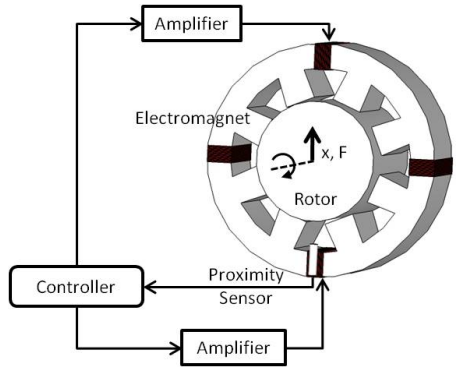

Figure 4: AMB rotor suspension.

to the CS and MS AMBs, respectively, the force F generated by the AMB acting on the rotor can be linearized to be,

$$F = K_x x + K_i i_c, \tag{4}$$

where x here corresponds to the rotor lateral displacement, and i_c is the control current to the AMB actuator. The open loop stiffness K_x for the MS and the CS AMBs are 1.27 M/mm and 2.26 N/mm, respectively. Similarly, the corresponding open loop gains K_i are 199.3 N/A and 265.86 N/A. The remaining electronic components closing the AMB control loop as shown in Fig. 4, such as proximity sensors and amplifiers, are later included in the AMB force calculation as low pass filters.

The final state space model of the rotor/AMB system has the form in Eq. (1), where the state vec-

tor is composed of the rotor modal states and the states of amplifiers, sensors and other electronics. Detail information on the system state space matrices can be found in [15].

4 Iterative LQG Controller Tuning for Lateral Rotor Suspension

Here we discuss the design procedure of the AMB lateral suspension LQG controller for the compressor test rig described in Sect. 3. In order to simplify the design process of the LQG controller, we initially ignore the effects of the gyroscopics and only consider a single control axis for the combined motor-side (MS) and compressor-side (CS) radial bearings.

An iterative process is employed for the selection of the LQG weights that would produce the controller with the best performance and stability margins. In the minimization of the LQG cost function, the optimization problem is sensitive to the ratio between the magnitudes of the penalty weights Q and R. Thus, the design problem can be simplified by fixing the value of one penalty weight, and studying how the remaining weighting matrix affects the performance of the resulting LQG controller. In the design of the AMB suspension controller for the test rig, we selected the weighting matrices to be,

$$R = I, \tag{5}$$

$$Q = q_y C^{\mathrm{T}} C + q_i I, \tag{6}$$

where the constant q_y is the weight on the system output and q_i is the variable to iterate upon. Then, the LQG cost function becomes

$$J_{\mathrm{LQG}} = E\left\{ \lim_{T\to\infty} \int_0^T \left(q_y y^{\mathrm{T}} y + q_i x^{\mathrm{T}} x + u^{\mathrm{T}} u \right) \mathrm{d}t \right\}. \tag{7}$$

We observe from Eq. (7) that q_i is the penalty on the system states. This corresponds to the states of the sensor and amplifier models included in the AMB system, as well as the modal states of the free-free rotor. The time constants of the amplifier and sensor models are small, and the state penalty in the LQG cost function will mostly affect how fast the rotor states settle. Therefore, the weight q_i has an important effect on how much the rotor modes are excited during the AMB control, and how fast they are damped when excited by external disturbances.

The ratio of the output weight q_y to the state weight q_i in Eq. (7) was found to play an important role in the trade-off between robustness and performance of the AMB suspension system. Given a sufficiently large weight on the AMB system outputs, the controller will put most of its effort in keeping these outputs near zero by "clamping" the rotor at the measurement points. This will result in no direct attenuation of the internal vibrations of the rotor modes, which could eventually lead to instability of the AMB system. On the other hand, if the weight on the output is too small when compared to the state weight, then the closed-loop response with the resulting LQG controller will be sluggish in order to avoid the penalty of exciting the rotor modes. For our design, the rotor was considered to be rigid, thus a larger emphasis was put on regulating the system outputs. A reasonable value of q_y was found to be 0.2 for the state weight q_i ranging from 0.01 to 100. Additionally, we assumed the noise level in both the control input and the feedback output signals to be 0.5% of the signal full scale (FS) and the noise in each channel to be independent. This gives us a covariance matrix for the noise input of

$$W_{\mathrm{n}} = \begin{bmatrix} 2\times 10^{-4} B^{\mathrm{T}} B & 0 \\ 0 & 2\times 10^{-4} \end{bmatrix}. \tag{8}$$

During the iterative design process of the LQG controller that we present here, twenty values of q_i were selected between 0.01 and 100. For each iteration step in this process, the value of q_i was increased and the optimal LQG regulator minimizing the cost function J_{LQG} was computed. The relevant robustness and performance characteristics of the closed-loop AMB system with the derived controller were determined for each value of q_i. This information was collected, and then presented at the end of the iterative loop for all values of q_i's to select the best state/output weight combination. Figure 5 demonstrates how the stability margins, the transient response, and the steady state characteristics of the LQG stabilized closed-loop system change as the state weight q_i is increased. The gain and phase margins are presented in Figs. 5(a) and 5(b), respectively, for the selected range of q_i. As the state weight is increased, a slight improvement in the stability margins can be initially observed due to the higher level of damping on the modes. However, as the value of q_i is further increased, both the gain and phase margins drop rapidly. The LQG controller becomes slow and sluggish due to the large penalty that results from exciting the rotor modal states.

A good transient response is generally required in an AMB system for a smooth transition between the different operating conditions of the rotating machine. Additionally, poor transient characteristics of the closed-loop system can be a warning flag for possible issues that could arise during the implementation of the feedback controller. The rise time, the settling time and the percentage overshoot corresponding to the step response at the motor-side and compressor-side AMBs are presented in Figs. 5(d), 5(e) and 5(f), respectively. As expected, both the rise time and the settling time tend to increase as the state weight increases and a larger penalty is given for exciting the rotor modes. By the same token, the overshoot of the step response decreases for the slower closed-loop system that results from increasing the value of q_i.

Two closed-loop characteristics in the ISO specifications that were monitored closely during design of the levitation controller are the peak magnitude of the sensitivity function and the peak vibration level in the unbalance response test. The change in these two values as a function of the state weight is presented in Fig. 6. The peak rotor displacement shown in Fig. 6(a) corresponds the forced response of the lateral suspension with an unbalance mass positioned at the rotor midspan. The size of the unbalance was selected to be $4U_{\mathrm{b}} = 4(6350W/N)$, following the API 617 specification [16] for axial and centrifugal compressors. The journal static load W and the maximum operating speed N are expressed in kg and rpm, respectively. The speed range in the unbalance response test is between zero and 30,000 rpm. The peak vibration level shown in Fig. 6(a) corresponds to the rotor maximum displacement at the system first critical speed Nc1. The peak displacement at this critical speed decreases as the damping on the system modes is increased together with the value of the state weight q_i. Based on the ISO 14839-2 standard, the vibration level of this machine is within Zone A specification for all the values of q_i considered here.

The peak magnitude of the sensitivity function shown in Fig. 6(b) is also considered important in the design of the AMB suspension controller. The ISO 14839-3 standard recommends a peak sensitivity value below 3 for new machines with AMBs. We observe from Fig. 6(b) that the closed-loop system with the LQG controller does not satisfy this requirement when the value of q_i is too large. This is in agreement with the drop in the gain margin observed in Fig. 5(a) for large values of q_i. The final value of the state weight was selected by considering all the trade-offs illustrated in Figs. 5 and 6. Stability margins, transient response and controller bandwidth were all considered in the selection of the best value of q_i. In this case, the value $q_i = 8.9$ was decided to give the best stability margin of the closed-loop system and a reasonable controller bandwidth for digital implementation. The final value of q_i is marked in the above mentioned figures by a vertical dashed line.

The LQG controller corresponding to the selected state weigh q_i has a total of 24 states. The order of the controller is then reduced in Matlab to 11 by employing the Hankel singular value

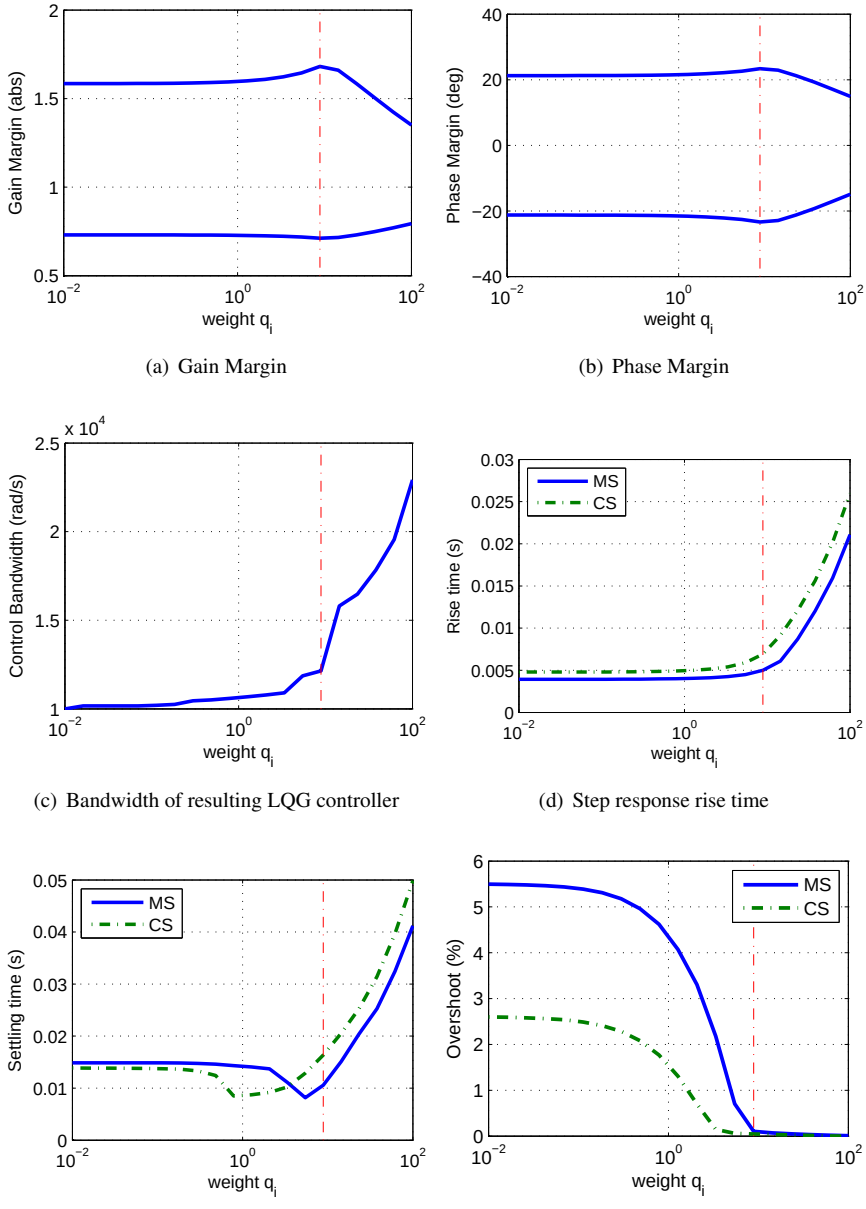

(a) Gain Margin

(b) Phase Margin

(c) Bandwidth of resulting LQG controller

(d) Step response rise time

(e) Step response settling time

(f) Step response overshoot

Figure 5: Results from the design iteration of the LQG radial AMB suspension controller.

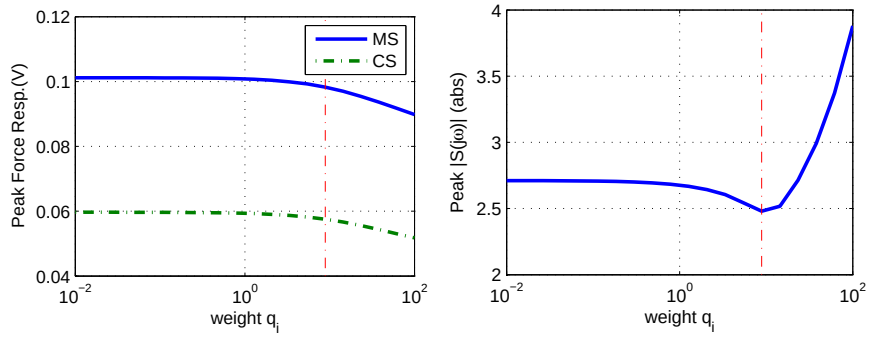

(a) Peak unbalance response vibration level (b) Peak magnitude of the sensitivity function

Figure 6: ISO vibration and stability margin measures for the design iteration of the LQG radial AMB suspension controller.

based model reduction function *reduce*. This reduction helps the implementation of the controller by eliminating unnecessary high frequency components of the controller. A simplified representation of the LQG-controlled system in terms of the closed-loop AMB stiffness is plotted on the critical speed map in Fig. 7. The bearing stiffness is defined to be the reaction force f to a disturbance in the rotor position x, which can be simplified for one control axis of a single radial AMB as,

$$F(s) = \left(K_i G_a(s) \left[K_{LQG}(s)\right]_{1\times 1} G_s(s) + K_x\right) X(s). \tag{9}$$

The transfer functions $G_a(s)$ and $G_s(s)$ represent the dynamics of the amplifier and sensor electronics, respectively. The controller equation $\left[K_{LQG}(s)\right]_{1\times 1}$ is here isolated to one axis of a single radial AMB by ignoring the cross-coupled terms between the bearings.

The unbalance response of the radial AMB system is presented in Fig. 8 based on the mathematical model of the system and the final LQG controller. Two separate cases were simulated, following the specification in API 617 [16] on the size and location of the unbalance forces. The unbalance forces were located along the rotor length to excite the rotor modes within or near the speed range of the machine. Figure 8(a) shows the rotor vibrations for a single unbalance mass of $4U_b$ at the rotor midspan. In this case, the rotor parallel mode corresponding to Nc1 is excited in the forced response at the critical speed near 7,050 rpm. The maximum amplification factor (AF) for this mode combining the motor-side and compressor-side vibration levels is 0.72, and thus it is considered critically damped by the API standard. Also, the peak rotor displacement at the critical speed is below 30% of the minimum clearance C_{min}, which would qualify the machine to be in Zone A as defined by the ISO 14839-2 standard.

The rotor vibration levels for unbalance masses of $4U_b$ located at each rotor end and separated by 180° in phase are shown in Fig. 8(b). In this case, the rotor conical mode is excited in the forced response, which corresponds to the second critical speed Nc2 near 8,600 rpm. The maximum amplification factor (AF) for this mode combining the motor-side and compressor-side vibration levels is 0.82, which is once again within the range corresponding to critically damped modes as specified by the API standard. The peak rotor displacement at the critical speed in this case is also below 30% of the minimum clearance C_{min}, and the machine would again qualify for Zone A as defined by the ISO 14839-2 standard.

As stated in [17], the ISO 14839-3 standard requires the magnitude of the sensitivity function to be below the maximum value of 3 to qualify for Zone A recommended for new machines with

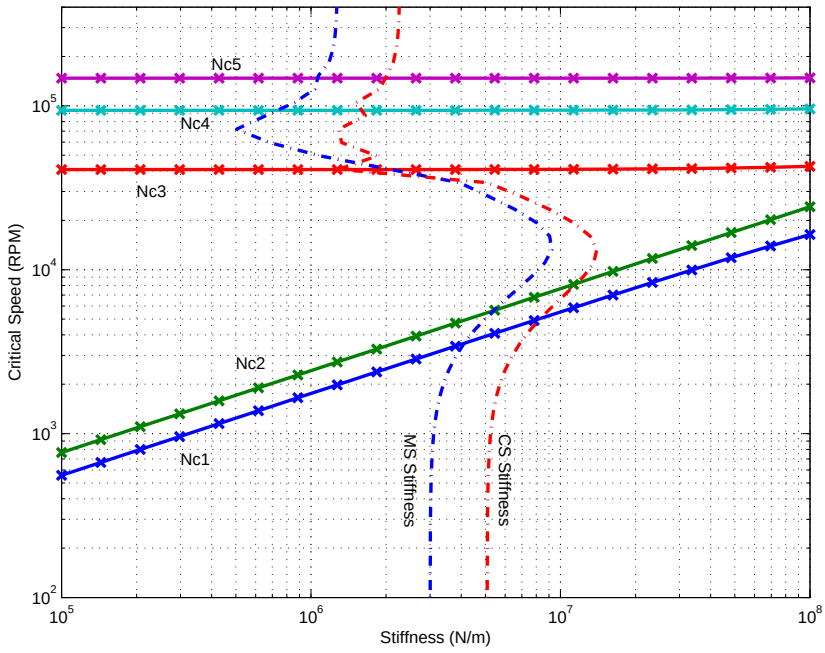

Figure 7: Closed-loop AMB stiffness with the LQG controller.

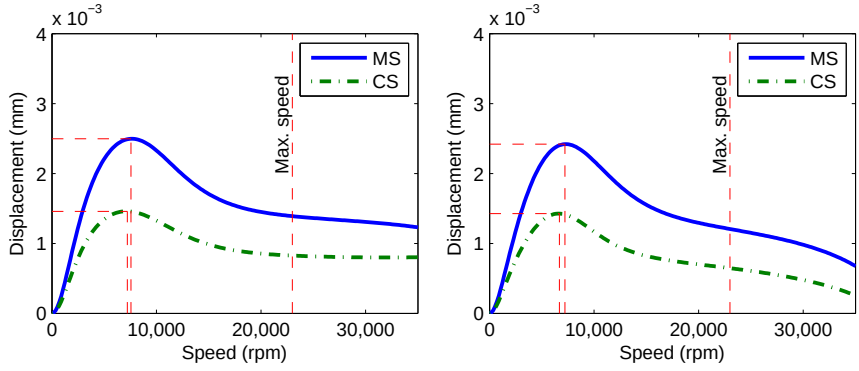

(a) Exciting Nc1 (b) Exciting Nc2

Figure 8: Simulated forced response with the unbalance mass as specified by API 617 [16].

AMBs. The magnitude plots of the sensitivity function with the LQG controller is presented in Fig. 9 based on the mathematical model of the system. Because of the gyroscopic effects acting on the rotor, the dynamics of the closed-loop AMB system varies at different operating speeds of the compressor. Therefore, the sensitivity function is plotted in Fig. 9(a) at zero speed, and the same function is presented in Fig. 9(b) for the maximum design speed as specified by the ISO specification. In both cases, the peak magnitude is less than 3, which qualifies the machine for Zone A.

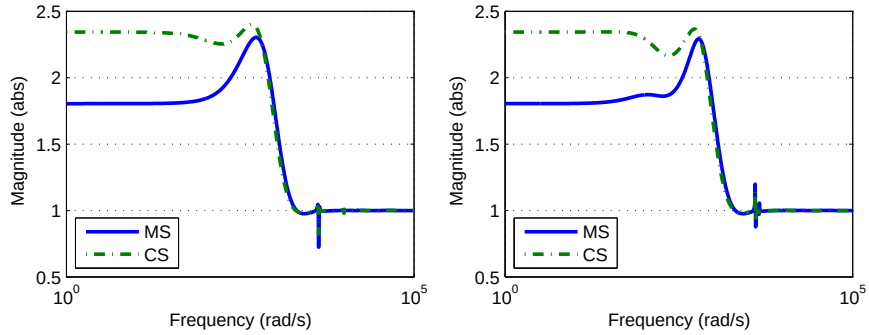

(a) 0 rpm (b) 23,000 rpm

Figure 9: Magnitude of the sensitivity function at zero and the maximum continuous speed.

5 Experimental Results

In the experimental implementation of the LQG controller, a small integrator term was added to each control channel to compensate for static disturbances such as the rotor weight. Because of the space limitation, here we present only the measurements at the compressor side bearing. The Bode plots of the radial AMB plant model are shown in Fig. 10 together with the measured plant frequency response from the experimental test rig. A good match is observed between the theoretical and the measured responses in both the magnitude and the phase curves. The experimental measurements clearly demonstrate that the rotor first bending mode (third critical speed) Nc3 is accurately captured in the mathematical model.

A comparison between the theoretical and the measured Bode plots of the closed-loop sensitivity function is presented in Fig. 11 for the static rotor. In this case, a good match is observed between the modeled and the actual system responses. The measured magnitude of the sensitivity function at the compressor side is below the limit for Zone A as defined in ISO 14839, which is recommended for all new machines with AMBs.

Finally, the measured rotor zero-to-peak vibration is shown in Fig. 12 for the radial AMB suspension system. The rotor vibrations at the motor-side and the compressor-side measurement points are recorded for the closed-loop system with the final LQG controller. The same rotor vibrations are recorded for the AMB system with a preliminary PID controller tuned for the initial levitation of the rotor. Although these two controllers may not be appropriate for direct comparison since the PID controller was only tuned for initial levitation, Fig. 12 clearly shows that the LQG controller provides significant improvements over the original PID controller in terms of rotor vibration. Particularly, it is seen that the vibration level at the motor-side with the PID controller exceeds the limit defined by ISO 14839 for Zone A. On the other hand, the LQG controller maintains the rotor vibration well within the recommended level for new machines with AMBs.

6 Conclusions

The design of an LQG controller for the AMB levitation system of a high speed compressor was presented in this paper. The iterative design process described in this paper searches over a range of LQG weights to find the optimal controller that performs best in the trade-off between stability robustness and performance. The controllers were designed to satisfy the recommendations in the

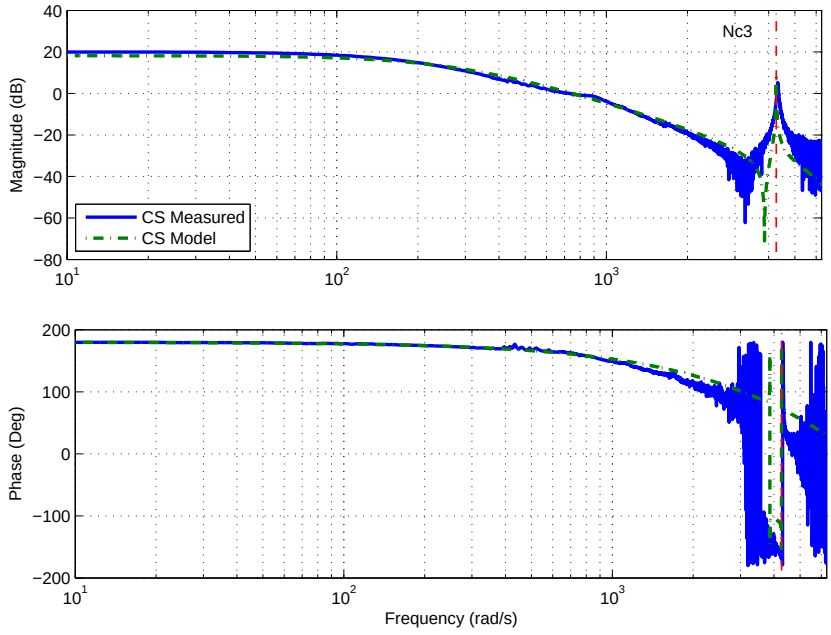

Figure 10: Bode plots of the lateral AMB plant model at the compressor-side (CS).

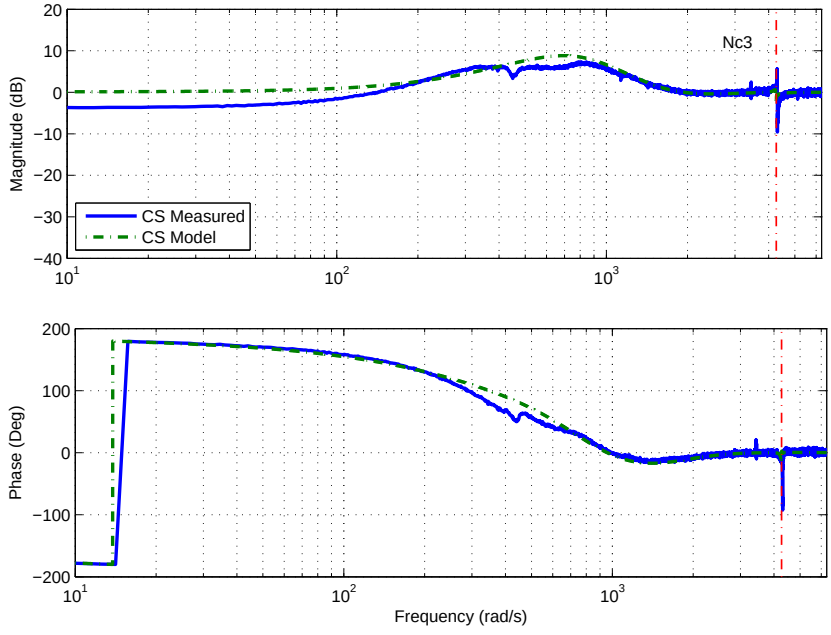

Figure 11: Bode plots of the lateral AMB sensitivity function at the compressor-side (CS).

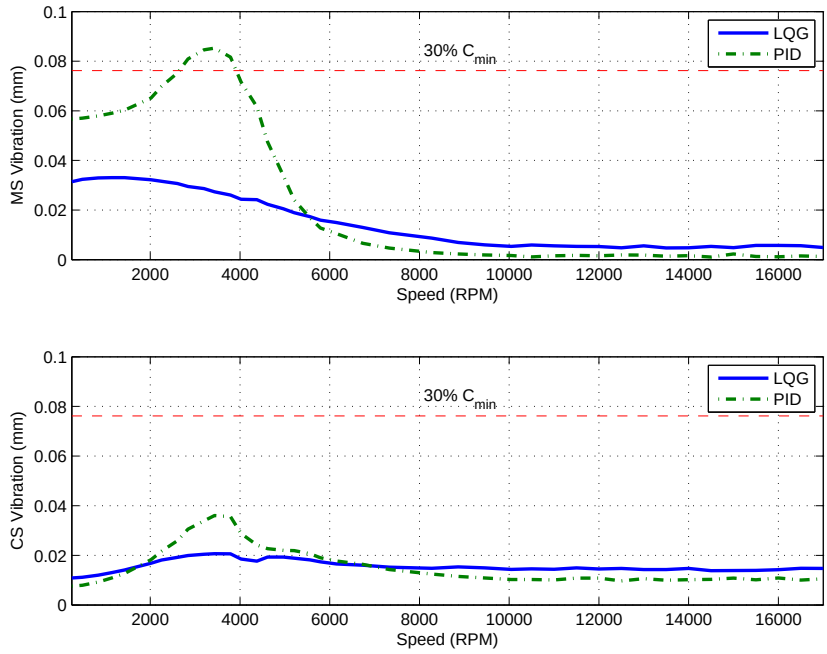

Figure 12: Experimental rotor vibration level vs. speed.

relevant ISO and API standards. The LQG controllers was designed to minimize the vibration due to the unbalance forces. The designed AMB controllers were implemented on the compressor test rig, and experimental measurements were presented to validate the theoretical design. The measured responses of the closed-loop AMB systems demonstrated satisfactory results. Experimental data showed that the API and ISO requirements on rotor vibration and system robustness were satisfied for this machine.

The controller design method presented in this paper has the advantage that it develops a sophisticate optimal controller, while keeping the human operator in the decision loop with very clear and specific feedback on how AMB system characteristics are affected by the chancgs in the controller parameter. Similarly to a PID controller, the operator can ”tune” the controller according to the desired closed-loop characteristics. This iterative tuning method was demonstrated in this paper to result in good performance and stability robustness for AMB systems with rigid rotors.

References

[1] S. Liu, X. Su, and L. Yu. Robust pid controller design for active magnetic bearing. In *Proc. of the 7th International Symposium on Magnetic Bearings*, pages 305–310, August 2000.

[2] T. Dimond, P. Allaire, S. Mushi, Z. Lin, and S. Y. Yoon. Modal tilt/translate control and stability of a rigid rotor on active magnetic bearings. *submitted to the J. of Dynamic Systems, Measurement, and Control*, 2012.

[3] J. Kim and D. C. Han. Robust centralized controller design for a rotor system supported by magnetic bearings. In *Proc. of the 3rd International Symp. on Magnetic Bearings*, pages 527–536, August 1992.

[4] T. Hu, Z. Lin, W. Jiang, and P. E. Allaire. constrained control design for magnetic bearing systems. *ASME J. of Dynamic Systems, Measurement, and Control*, 127:601–616, 2005.

[5] G. Li. *Robust Stabilization Of Rotor-Active Magnetic Bearing Systems*. PhD thesis, University of Virginia, 2006.

[6] S. Mushi. An active magnetic bearing test rig for aerodynamic crosscoupling: Control design and implementation. Master's thesis, Univeristy of Virginia, 2008.

[7] Z. Gosiewski and Falkowski. Two-axial gyroscope with magnetically supported rotor. In *Proceedings of the 5th International Symposium on Magnetic Bearings*, pages 65–70, 1996.

[8] L. Zhao, K. Zhanga, R. Zhu, and H. Zhao. Experimental research on a momentum wheel suspended by active magnetic bearings. In *Proceedings of the 8th International Symposium on Magnetic Bearings*, pages 605–609, 2002.

[9] S. Y. Yoon, Z. Lin, T. Dimond, and P. E. Allaire. Control of active magnetic bearing systems on non-static foundations. In *Proceedings of the 9th IEEE International Conference on Control and Automation (ICCA)*, pages 556–561, December 2011.

[10] W .Grega and P. Adam. Comparison of linear control methods for an amb system. *International Journal of Applied Mathematics and Computer Science*, 15:245–255, 2005.

[11] H. J. Ahn, S. W. Lee, S. H. Lee, and D. C. Han. Frequency domain control-relevant identification of mimo amb rigid rotor. *Automatica*, 39:299–307, 2003.

[12] R. P. Jastrzebski and R. Pollanen. Compensation of nonlinearities in active magnetic bearings with variable force bias for zero and reduced-bias operation. *Mechatronics*, 19:629–638, 2009.

[13] Zhuravlyov Y. N. On lq-control of magnetic bearing. *IEEE Transactions on Control Systems Technology*, 8:344–350, 2000.

[14] K. Zhou, J. C. Doyle, and K. Glover. *Robust and Optimal Control*. Prentice Hall, N.J., USA, 1996.

[15] S. Y. Yoon, Z. Lin, and P. Allaire. *Control of Surge in Centrifugal Compressors by Active Magnetic Bearings*. Springer-Verlag, 2012.

[16] American Petroleum Institute, Washington, DC. *API 617: Axial and Centrifugal Compressors and Expander-compressors for Petroleum, Chemical and Gas Industry Service*, 7th edition, July 2002.

[17] International Organization for Standardization. *ISO 14839-3: Mechanical vibration - Vibration of rotating machinery equipped with active magnetic bearings - Part 3: Evaluation of stability margin*, 2006.